STUDY OF HYPERFRAGMENTS

Part V. Analysis of Light Hyperfragments

BY K. N. CHAUDHARI, S. N. GANGULI, N. K. RAO AND M. S. SWAMI*

(Tata Institute of Fundamental Research, Bombay, India)

Received September 28, 1966

(Communicated by Dr. R. R. Daniel, F.A.SC.)

ABSTRACT

464 non-mesic and 65 mesic decay of hyperfragments (HFs) produced by pions of momenta 3·5 GeV/c. and 17·2 GeV/c. and protons of momentum 23 GeV/c., have been used to obtain information on Q^-, the ratio of non-mesic to π^- mesic events and S, the ratio of neutron to proton stimulated events as a function of charge of HFs. Q^- is found to increase rapidly with the increase in charge of HFs; the value of Q^- for HFs of $Z \geqslant 3$ is $14{\cdot}6 \pm 3{\cdot}0$ which is high compared to the theoretical value of about 4 to 5. The value of S is found to be > 1 for all HFs of $Z \geq 2$.

1. INTRODUCTION

THE common decay modes of hyperfragments (HFs) are: (i) mesic decay (MHFs) in which a pion is emitted, and (ii) non-mesic decay (NMHFs) in which no pion is emitted. The latter decay mode is predominantly due to the interaction of Λ with a single nucleon which can be written as:

$$\Lambda + p \rightarrow p + n \tag{1}$$

$$\Lambda + n \rightarrow n + n. \tag{2}$$

Reaction (1) is called the stimulation of Λ by a proton and reaction (2) is called the stimulation of Λ by a neutron. The experimentally determinable parameters in the decay of HFs are:

$$(a)\ Q^- = \frac{\text{number of NMHFs}}{\text{number of MHFs that decay by } \pi^- \text{ mode}}$$

$$(b)\ S = \frac{\text{number of NMHFs that decay without emission of fast proton}}{\text{number of NMHFs that decay with emission of fast protons}}.$$

* Now at the Physics Department of Punjab University, Chandigarh, India, on deputation from the Tata Institute of Fundamental Research.

In case (*b*), fast protons are defined as those that have energy $\geqslant 30$ MeV; this energy criterion removes the unwanted contribution of charged particles due to evaporation of the HF core nucleus.

In order to understand the A-nucleon interaction it is of importance to investigate experimentally the ratios Q^- and S as a function of charge and mass of HFs. These ratios have been theoretically calculated by Dalitz[1] and Ferrari and Fonda[2] respectively; a comparison of the theoretical values with those of the experiment will provide valuable information on $\wedge$-nucleon interaction. Since accurate mass or charge determination is not possible for short-range HFs, we have selected for this investigation only those HFs that have ranges $> 20\,\mu$m.

2. Experimental Details and Results

2.1. *Details of the Stacks*

Three nuclear emulsion stacks A, B and C which were exposed to beams of 3·5 GeV/c. pions, 23 GeV/c. protons and 17·2 GeV/c. pions respectively have been used in this investigation. The details regarding the stacks, scanning and selection criteria of HFs are described in Parts I, II and IV[3–5] of this series.

For accurate analysis of the events, it is necessary to know the shrinkage factor and stopping power of the emulsions. These have been obtained in the following way:

Stacks B and C.—The thickness of emulsions in stacks B and C were measured before and after processing of the stacks; therefore the shrinkage factor for these emulsions was known. Stopping powers of stacks B and C were determined by measuring in each the ranges of 50 flat μ^+ arising from π^+ decay at rest. The mean ranges of μ^+ in these two stacks were found to be $601{\cdot}4 \pm 3{\cdot}5\ \mu$m and $605{\cdot}0 \pm 3{\cdot}0\,\mu$m respectively. These are in good agreement with the mean range of $602{\cdot}2 \pm 1{\cdot}5\,\mu$m,[6] obtained for μ^+ in a standard emulsion of density 3·815 gm./cm.^{3}

Stack A.—The original thicknesses of the emulsion pellicles of stack A were not known. Therefore the shrinkage factor and the stopping power were determined by 'regression method' of Fry and White[7] using 50 μ^+ from decay of π^+ mesons at rest. With this method, the mean range of μ^+ was found to be $612 \pm 5\ \mu$m; this value lies within two-standard deviation for the μ^+ range in a standard emulsion.

Since the stopping powers for the three stacks A, B and C are in agreement with that of a standard emulsion, the range-energy relations given by Heckman *et al.*[8] for standard emulsion were used throughout.

2.2. *Selection of Events*

A total of 1173 HFs were obtained in the three stacks. From this we have selected those HFs that have ranges > 20 μm. With this procedure we have obtained in all 464 NMHFs and 67 MHFs. The number of black and grey tracks (N_h) associated with each parent star containing the HF was determined. From the N_h distribution of these stars, it was concluded that more than 90% of the HFs were produced in disintegrations of heavy nuclei (Ag, Br) of emulsion.

Data collected on the range distribution of HFs as a function of range for various incident beams[9–11] including the results from the present investigation are given in Table I. It can be seen from this table that as the energy of the incident beam increases the fraction of long range HFs also increases. This clearly brings out the advantage of working with high energy incident beams which result in easier identification of HFs.

TABLE I

Ranges of hyperfragments (in percentage) for different incident beams

	Incident beam	Percentage of HFs with range			
		0–10 μm	10–20 μm	20–50 μm	>50 μm
	Stopping K^-[9]	61·6*	10·0	11·6	16·8
	0·8 GeV/c. K^-[10]	85·0	2·6	3·4	9·0
	3·0 GeV/c. K^-[11]	74·4	6·0	5·5	14·1
	5·0 GeV/c. K^-[11]	72·9	6·5	6·7	13·9
Present work	3·5 GeV/c. π^-	67·6	11·9	9·1	11·4
	17·2 GeV/c. π^-	36·3	13·2	17·8	32·7
	23 GeV/c. P	35·0	14·3	20·0	30·7

* HFs of range ≤ 1 μm are not included in this.

2.3. *Mass determination of Particles from Decay of HFs*

All tracks from decay of HFs were followed till they were brought to rest, left the stack or interacted in flight. Identification of pions from decay of HFs was made from the variation in grain density and Coulomb scattering along their tracks. In this way all the MHFs were identified. In NMHF events mass measurements were made on all fast charged particles of residual range $\geqslant 4$ mm. and which subtended dip-angles $\leqslant 30°$ with respect to the plane of emulsion; there were 57 such tracks. In these cases mass measurements were carried out by the constant Sagitta scattering method for stopping particles; the scheme used was P (0·7 μm). From a comparison of these data with similar measurements made on well-identified protons, it is found that all the 57 fast-charged particles except 2 are due to protons; these two tracks could be due to deuterons or tritons (the details regarding this type of measurement is described in Part III.[12] Thus we conclude that the contribution of deuterons and tritons among the fast-charged particles of range $\geqslant 4$ mm. is $\lesssim 4\%$.

2.4. *Charge Spectrum of HFs*

The charge of a particle producing a track of range $> 20\,\mu$m can be found in two ways: (*a*) by track width measurement and (*b*) by visual inspection. They are described below.

(*a*) *Track-width method.*—Track-width measurements have been made on well identified flat (dip-angle $\leqslant 10°$) protons, alpha-particles, Li^8 and B^8 tracks. The variation of track-width as a function of residual range is shown in Fig. 1 (*a*). The variation of track-width with dip-angle of the tracks of Li^8 fragments of range 60 μm is shown in Fig. 1 (*b*). From Fig. 1 it is clear that the average track-width for tracks of dip-angles $\leqslant 25°$ remains constant. With this method we have made track-width measurements on all tracks of HFs, whose dip-angles were $\leqslant 25°$. The typical errors involved in the charge

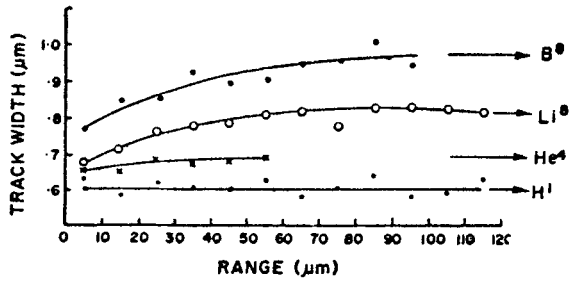

FIG. 1. (*a*) Track-width *versus* residual range for protons, alphas, Li^8 and B^8 tracks.

estimation by this method are: (i) 0·5 charge unit for tracks of range $> 60\,\mu$m and (ii) 1·0 charge unit for tracks in the range interval 20–60 μm.

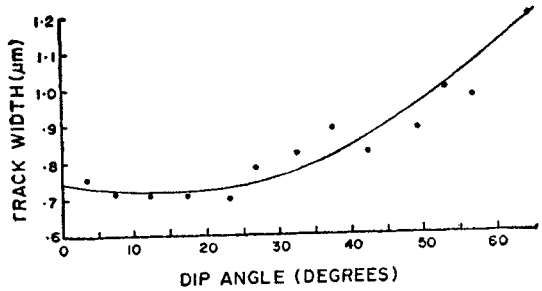

FIG. 1. (*b*) Variation of track-width, for Li^8s of range = 60 μm, as a function of dip-angle.

(*b*) *Visual estimation of charges.*—In this method the charge of a fragment was estimated by visually comparing it with well identified fragments of comparable range and dip-angle. The charge of the HF was determined by visually inspecting the HF track and also its secondary decay products. This method is particularly useful when the HF track is quite steep and the track-width is difficult to perform. The error in the charge estimation is on the average one charge unit.

The charges of HFs, estimated by the above two methods, were compared, whenever possible, with the charges of uniquely identified HFs. The uniquely identified HFs were those, which gave correct binding energies and no other decay scheme was possible for the events (*see* Section 2.5 for analysis of these events). When the charge estimate for the HFs is not unique, equal weightage is given for the assigned charges of the HFs. In this way visual estimation of charge of HFs is found to be good in $\approx$90% of the cases. The charge spectrum of HFs obtained is shown in Fig. 2. The hatched portion of the histogram refers to mesic decay of HFs and the rest to non-mesic decay of HFs*.

2.5. *Analysis of Hyperfragments*

(*a*) *Decay modes of π^- mesic HFs.*—Out of the 65 MHFs† obtained in this investigation only in 44 cases the pion could be brought to rest; in the remaining cases the pions left the stack or interacted in flight. In order to fit decay schemes the events were analysed on CDC-3600 computer. For

* Possible cases of eleven π^0 emission in the decay of HFs were not included in this histogram for NMHF decays.

† Two HFs that decayed by μ^- and π^+ modes are not included in this analysis; see reference [18].

this purpose the identity of the meson track was assumed to be due to a negative pion; as for the charges of the other prongs and that of HF track the maximum and minimum values permissible within the measuremental errors were assigned. All possible combinations for the decay schemes were then attempted by the computer. The unbalanced momentum was given to an invisible recoil or a neutron; if the unbalanced momentum was less than 100 MeV/c., the computer also tried decay schemes without any invisible recoil or neutron. The computer printed out all possible decay schemes where binding energies of HFs agreed to within three-standard deviation of the expected binding energies. In all these computations the mass values of various nuclei and particles were taken from Konig *et al.*,[14] and Rosenfeld *et al.*[15]

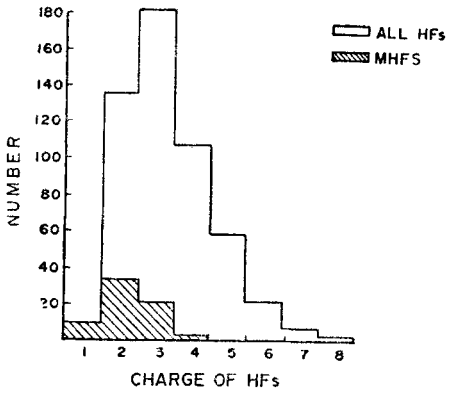

FIG. 2. The charge spectrum of HFs. The hatched portion refers to π^- mesonic HFs.

With the above computer analysis we could obtain unique decay schemes for 32 MHFs. Decay schemes and binding energies for these events are presented in Table II. These binding energies are in good agreement with those quoted by Burhop *et al.*[17]

(*b*) *Decay modes of non-mesic HFs.*—All non-mesic HFs have also been analysed by the CDC-3600 computer in the same way as is described in Section 2.5 (*a*); besides all that is described in 2.5 (*a*), the computer also tried decay schemes with a neutral pion whenever the total visible energy was $\leqslant$ 10 MeV.‡ In this way 11 possible π° decays and 25 unique non-mesic decays have been identified; they are presented in Tables III (*a*) and III (*b*) respectively.

‡ An upper limit of 10 MeV has been chosen because it is known from mesic HFs that the total energy carried away by secondary charged particles other than the pion is, in general, $\leqslant$ 10 MeV.

TABLE II

Decay schemes of uniquely identified mesic hyperfragments

Hyperfragment	Decay mode	No. of events	$\bar{B}_\Lambda \pm \Delta B_\Lambda$ (MeV)
${}_\Lambda H^3$	$\pi^- + H^1 + H^1 + n$	1	$0{\cdot}38 \pm 0{\cdot}48$
	$\pi^- + He^4$	1	$3{\cdot}06 \pm 0{\cdot}98$
${}_\Lambda H^4$	$\pi^- + H^1 + H^3$	1*	$1{\cdot}86 \pm 0{\cdot}52$
	$\pi^- + He^3 + n$	1	$1{\cdot}86 \pm 1{\cdot}26$
${}_\Lambda He^4$	$\pi^- + H^1 + He^3$	1	$2{\cdot}8 \pm 0{\cdot}58$
${}_\Lambda He^5$	$\pi^- + H^1 + He^4$	11	$2{\cdot}61 \pm 0{\cdot}17$
		3*	$2{\cdot}97 \pm 0{\cdot}51$
${}_\Lambda He^7$	$\pi^- + H^3 + He^4$	1	$2{\cdot}29 \pm 0{\cdot}75$
	$\pi^- + H^2 + He^4 + n$	1	$4{\cdot}17 \pm 3{\cdot}72$
	$\pi^- + H^1 + Li^6$	1	$5{\cdot}24 \pm 0{\cdot}50$
${}_\Lambda Li^7$	$\pi^- + He^3 + He^4$	1	$5{\cdot}96 \pm 0{\cdot}41$
	$\pi^- + H^1 + H^2 + He^4$	1	$5{\cdot}95 \pm 0{\cdot}45$
	$\pi^- + He^4 + He^4$	2	$5{\cdot}48 \pm 0{\cdot}55$
${}_\Lambda Li^8$	$\pi^- + H^1 + Li^7$	1	$5{\cdot}16 \pm 0{\cdot}78$
	$\pi^- + H^1 + H^1 + He^6$	1	$6{\cdot}48 \pm 0{\cdot}25$
${}_\Lambda Li^9$	$\pi^- + H^3 + Li^6$	1	$7{\cdot}11 \pm 0{\cdot}73$
	$\pi^- + He^4 + He^4 + n$	1	$7{\cdot}41 \pm 0{\cdot}89$
${}_\Lambda Be^{7+}$	$\pi^- + H^1 + H^1 + H^1 + He^4$	1	$4{\cdot}66 \pm 0{\cdot}59$
${}_\Lambda Be^9$	$\pi^- + H^1 + H^1 + Li^7$	1	$6{\cdot}82 \pm 0{\cdot}15$

* These events are from stack A.

\+ For details *see* Chaudhari *et al.*[16]

2.6. *Fast Proton Spectrum*

It was shown in Section 2.3 that the contribution of deuterons and tritons amongst fast-charged particles is negligibly small ($\lesssim 4\%$). Therefore assuming that all fast-charged particles are protons, we have obtained the energy spectrum of fast protons (≥ 30 MeV) as a function of charge of HFs which

TABLE III (*a*)

Decay schemes of uniquely indentified π° mesic HFs

Hyperfragment	Decay mode	No. of events	$\bar{B}_\Lambda$* (MeV)
${}_\Lambda He^4$	$H^1+H^3+\pi^\circ$	5	0·6
${}_\Lambda Li^7$	$H^3+He^4+\pi^\circ$	2	6·5
${}_\Lambda Be^7$	$H^1+Li^6+\pi^\circ$	1	4·8
	$He^3+He^4+\pi^\circ$	1	2·6
${}_\Lambda Be^8$	$He^4+He^4+\pi^\circ$	1	5·8
${}_\Lambda B^9$	$H^2+Be^7+\pi^\circ$	1	5·3

* Errors in binding energies are not quoted for these events because they are quite large; errors are of ~10–20 MeV.

is given in Fig. 3. It is clear from this figure that the energy spectrum of fast protons is independent of the charge of HFs.

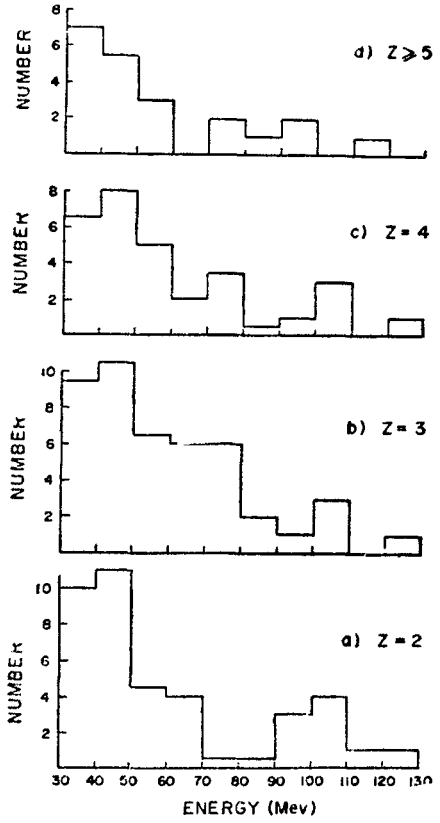

FIG. 3. Fast proton spectrum for HFs of charge, Z = 2, 3, 4 and ≥ 5.

TABLE III (*b*)

Decay schemes of uniquely identified NMHFs

Hyperfragment	Decay mode	No. of events	$\bar{B}_\Lambda \pm \Delta\bar{B}_\Lambda$ (MeV)
${}_\Lambda He^4$	H^1+H^2+n	3	0·9*
${}_\Lambda He^5$	H^1+H^3+n	7	4·4 ± 0·6
	H^2+H^2+n	2	1·0*
${}_\Lambda Li^7$	H^3+He^3+n	1	4·2*
	$H^1+H^3+H^3+n$	1	5·6 ± 1·7
${}_\Lambda Li^8$	$H^2+H^2+H^3+n$	1	4·6*
	H^1+He^6+n	1	6·8 ± 3·6
	$H^1+H^1+He^4+n$	1	6·06 ± 1·36
${}_\Lambda Be^{7+}$	$H^1+H^2+H^1+H^2+n$		7·39 ± 1·49
	or	1	
	$H^1+H^2+H^2+H^1+n$		4·54 ± 1·64
${}_\Lambda Be^8$	$H^1+H^2+He^4+n$	1	7·7 ± 6·1
	H^1+Li^6+n	1	8·7*
${}_\Lambda Be^9$	$H^1+H^1+He^6+n$	1	6·31 ± 1·34
${}_\Lambda Be^{10}$	$H^1+H^2+He^6+n$	3	9·47 ± 0·26
${}_\Lambda C^{12}$	$H^1+H^1+Be^9+n$	1	12·05*

* Errors in binding energies are not quoted for these events because they are quite large; errors are of 10–20 MeV.

+ For details *see* Chaudhari *et al.*[16]

3. DISCUSSION OF THE RESULTS

3.1. *Mechanism of Production of Light Hyperfragments*

A means of understanding the mechanism of production of light hyperfragments is by comparing their range distribution with that of ordinary light fragments, which are produced mostly in the cascade-evaporation stage of the disintegrating heavy nuclei (Ag and Br). Among the oridnary light fragments, identification of Li^8 can be made unambiguously because of the presence of two collinear alpha-tracks at their stopping end. Therefore we determined the range distribution for 800 Li^8 fragments obtained in the

TABLE IV (*a*)

Q^- and S as a function of charge

Charge of HF	2	3	4	$\geqslant 5$
Q^-=NMHF/MHF	$3{\cdot}0\pm0{\cdot}6$	$7{\cdot}6\pm1{\cdot}8$	$34{\cdot}7\pm20{\cdot}5$	$\gtrsim 87$
$S=\Lambda n/\Lambda p$	$1{\cdot}6\pm0{\cdot}9$	$\rightarrow 2{\cdot}4\pm0{\cdot}4$	$2{\cdot}4\pm0{\cdot}5$	$2{\cdot}6\pm0{\cdot}6$

TABLE IV (*b*)

Non-mesic to π^- mesic ratio (theoretical)

Hyperfragment	${}_\Lambda H^4$	${}_\Lambda He^4$	${}_\Lambda He^5$	${}_\Lambda Li^7$	${}_\Lambda Be$	${}_\Lambda C^{13}$
Q^-	0·15	0·5	1·8	2·7	6·2	11·3

present three stacks. The range distribution of all identified $Z = 3$ hyperfragments and that for the normalised Li^8 fragments is shown in Fig. 4. It is seen from this figure that the range distribution of hyperfragments with $Z = 3$ is quite similar to that of Li^8 fragments. From this we infer that light

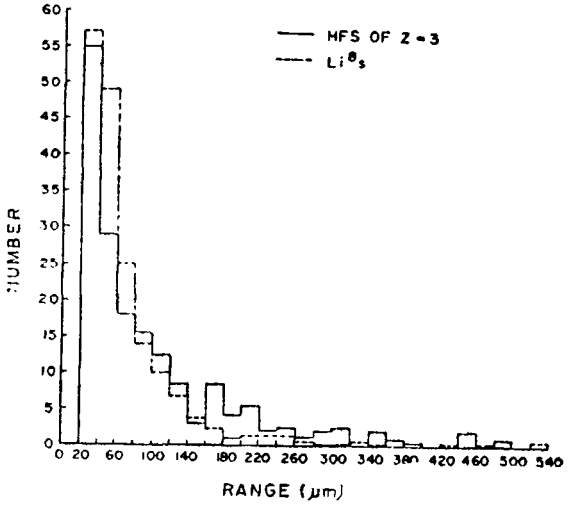

FIG. 4. Range distribution of HFs of Z = 3 and that of Li^8s. — refers to HFs of Z = 3. .....refers to Li^8s.

hyperfragments are mainly produced in the cascade-evaporation stage of disintegrating Ag and Br nuclei of emulsion. Similar conclusions have been drawn by Gagarin and Ivanova[18] and Cüer[19] from their work on production of light HFs by high energy particles ($E > 3$ GeV).

3.2. *The Ratio Q^-*

In Table IV (*a*) is presented the values of Q^-, the ratio of non-mesic HFs to π^--mesic HFs, as a function of charge. In Table IV (*b*) is given the values of Q^- from the theoretical calculation of Dalitz.[1] We now discuss separately the Q^- values for HFs of $Z = 2$ and $Z \geqslant 3$.

Helium HFs.—We see from Table IV (*a*) that the experimentally obtained value of Q^- for $Z = 2$ HF is $3{\cdot}0 \pm 0{\cdot}6$, whereas the calculated value from Table IV (*b*) for ${}_{\Lambda}He^5$ is $1{\cdot}8$. The small difference between the two values can be understood in the following way: Since the doubly charged HFs are a mixture of ${}_{\Lambda}He^{4,5,7}$, it is not possible to compare directly the experimental Q^- value for ${}_{\Lambda}He$ HFs with that of calculated one for ${}_{\Lambda}He^5$. It is seen from Table IV (*b*) that the calculated Q^- value for ${}_{\Lambda}He^4$ is $0{\cdot}5$; the value for ${}_{\Lambda}He^7$ is expected to be larger when compared with that of ${}_{\Lambda}He^5$. Therefore with the proper weightage of various species of He HFs, the Q^- value for ${}_{\Lambda}He$ HF is not expected to be very much different from that of ${}_{\Lambda}He^5$; the present experimental result within statistical error agrees with this expectation.

HFs of $Z \geqslant 3$.—It is seen from Tables IV (*a*) and IV (*b*) that the experimental values of Q^- for HFs with $Z \geqslant 3$ are quite large compared to the expected values from theoretical calculation. This difference cannot be understood from the explanation mentioned earlier for helium HFs; nor can it be accounted for by any type of experimental biases, namely the scanning loss of mesic hyperfragments of $Z \geqslant 3$, because it looks rather improbable that high charged MHFS could be missed while non-mesic ones are not. Further the charge estimation of the HFs cannot be in serious error because they have long enough residual ranges for their identification (the average range of these HFs is $\approx 90\,\mu$m). Among the NMHFs there can be some loss due to non-inclusion of one prong type of events. But this loss is expected to be small because light HFs, in general, will break up completely. Therefore the results presented in Table IV (*a*) are expected to represent the true situation and so there is a strong evidence that the theoretical values of Q^- for HFs of $Z \geqslant 3$ are really underes imated.

A study of Q^- values for HFs of $Z \geqslant 3$ has also been made by several authors.[20–25] All these values are quoted in Table V. Values of Q^- obtained by Schneps *et al.*,[20] Silverstein,[21] Sacton[22] and Bhowmik *et al.*[23] are from

HFs of all ranges. It is known that majority ($\geqslant 80\%$) of these HFs have ranges $\leqslant 20\,\mu$m; therefore the charge estimates are likely to have large errors. The values of Q^- quoted by Holland[24] and Kenyon *et al.*,[25] are comparatively very low; it might be possible that their low values are due to poor statistics. Since statistics in the present work is very good and only long-range HFs (RHF $> 20\,\mu$m) are used, we consider the value of Q^- which is $14{\cdot}6 \pm 3{\cdot}0$ for HFs of charge $Z \geqslant 3$, as the best value so far determined.

TABLE V

Non-mesic to mesic ratio for HFs with $Z \geqslant 3$

Reference	Primary beam used	Selection of HFs	Total No. of HFs with $Z \geqslant 3$	$Q^- = \frac{\text{N MHFs}}{\pi^- \text{ MHFs}}$
Schneps *et al.*[20] ..	Cosmic rays, Stopping K^-, a few GeV π^- & a few GeV P	All ranges*	175	$42{\cdot}7 \pm 21{\cdot}6$
Silverstein[21] ..	4·5 GeV π^-	(i) All ranges* (ii) Computer analysis	120	$16{\cdot}1 \pm 6{\cdot}3$
Sacton[22] ..	Stopping K^-	(i) All ranges* (ii) Computer analysis	75	$9{\cdot}7 \pm 3{\cdot}9$
Bhowmik *et al.*[23] ..	Stopping K^-	(i) HFs of all ranges (ii) Manual analysis (iii) Charge by visual estimation	29·8	15·5
Holland[24] ..	Stopping K^-	(i) $3{\cdot}3 < R_{HF} \leqslant 20\,\mu$m (ii) Analysis of production and decay vertices by computer	126	$3{\cdot}2 \pm 0{\cdot}7$
Kenyon *et al.*[25] ..	800 MeV/c K^-	(i) $R_{HF} \geqslant 40\,\mu$m and dip $\leqslant 60°$ (ii) Profile measurement	~30	2·4 to 5·0
Present work ..	3·5 GeV/c π^-, 17·2 GeV/c π^- and 23 GeV/c P	(i) $R_{HF} \geqslant 20\,\mu$m (ii) Profile measurement (iii) Computer analysis	376	$14{\cdot}6 \pm 3{\cdot}0$

* Majority of these HFs (*i.e.*, $\gtrsim 80\%$) are of range $\leq 20\,\mu$m.

3.3. *Stimulation Ratio S*

It has been shown by Burte *et al.* (Part III)[12] that among light HFs (i) Stimulation process by Λ-multinucleon interaction is negligible compared to that by Λ-single nucleon interaction, (ii) the percentage of HFs with two fast protons decreases from 3·9 to 1·1, when energies of both the fast protons

increase from 20 to 30 MeV, thereby decreasing the contribution of final-state and multinucleon interactions when the energy of fast proton increases from 20 to 30 MeV, and (iii) the emission probability of fast proton due to secondary collision process within the HF itself is almost zero. From the above observations it can be seen that the emission of a fast proton with energy $\geqslant$ 30 MeV from the decay of HF will arise almost exclusively due to $\wedge$-single proton stimulation process. One cannot obviously go on increasing

TABLE VI

$\wedge$-Neutron to $\wedge$-proton stimulation ratio

Reference	Primary beam used	Selection of HFs	No. of HFs used in analysis	Cut off energy of fast proton (MeV)	S= Neutron to proton stimulation ratio
Baldoceolin *et al.*[27] ..	4·5 GeV π^-	(i) Z=2, 3, 4 (ii) RHF$\geqslant$20 μm (iii) 2 or more prongs vertex	31	30	1·4
Silverstein[21] ..	4·5 GeV π^-	RHF$\geqslant$20 μm statistical analysis gives 185±40 HFs	56 185±40	30 40 30 40	0·9±0·3 1·4±0·5 0·9±0·2 1·7±0·3
Berkovich *et al.*[28] ..	4·5 GeV π^-	(i) RHF$\geqslant$20 μm (ii) Profile of connecting track	18	26	1·35
Sacton[22] ..	K^- at rest	All HFs except one prong events accepted (i) Computer analysis (ii) Statistical analysis to determine background	55	30	0·83±0·11
Bhowmik *et al.*[23] ..	Stopping K^-	(i) HFs of all ranges (ii) Scattering on secondaries (iii) Analysis manually (iv) Charge by visual estimation	41	30	0·42±1·4
Gorge *et al.*[29] ..	(i) K^- in flight (85 MeV) (ii) K^- at rest	(i) Track profile (ii) Scattering (iii) Computer analysis HFs of all ranges	22	30	2·3±1·1
Present work ..	3·5 GeV/c π^-, 17·2 GeV/c π^- & 23·0 GeV/c P	(i) HFs of $R_{HF}\geqslant$20 μm (ii) Constant sagitta on fast secondaries (iii) Computer analysis (iv) Charge estimate by profile and visual	453	30	2·3±0·24

the above energy criterion for a fast proton, because in that case $\wedge$-P stimulation type of events will be underestimated. Even with the 30 MeV cut-off energy criterion it is possible that $\wedge$-P stimulation type of events are underestimated; it is estimated that $\lesssim 10\%$ of $\wedge$-P stimulation process[26] will give rise to a proton of energy < 30 MeV. Since this percentage is small we assume that all those HFs which do not decay with the emission of a fast proton of energy $\geqslant 30$ MeV, are due to $\wedge$-single neutron stimulation process. Thus we define the stimulation ratio S, as the number of NMHFs that decay without the emission of a fast proton to those that decay with the emission of a fast proton of energy $\geqslant 30$ MeV. Values of S as a function of charge of HFs are presented in Table IV (*a*). The overall value of S for HFs of $Z \geqslant 2$ is $2{\cdot}3 \pm 0{\cdot}24$. A rough estimate of n/p of the core of HFs with $Z \geqslant 2$ is made from isotopic composition of HFs; this estimate is $\approx 1{\cdot}1$. Thus it is seen that even after taking into account the number of neutrons to protons in the core of HFs, the ratio S is > 1; this implies according to Ferrari and Fonda[2] that the stimulated decay takes place when the hyperon is in the Σ-state.

Several attempts in the past have been made by various authors[21–23, 27–2] to estimate the value of S. All these values are quoted in Table VI. Values of S obtained by Sacton,[22] Gorge *et al.*[29] and Bhowmik *et al.*[23] are based on HFs of all ranges; the majority of these HFs ($\geqslant 80\%$) have ranges $\leqslant 20\,\mu$m. Values of S obtained by Baldo-Ceolin *et al.*,[27] Silverstein[21] and Berkovich *et al.*,[28] for HFs of range $\geqslant 20\,\mu$m. are > 1, though the statistics is poor. In the present work which is based on 453 HFs of range $\geqslant 20\,\mu$m the value of S is found to be > 1 and is the best value so far available.

4. Conclusions

From the analysis of light hyperfragments, the following conclusions are drawn:

(i) By comparing the range distribution of $Z = 3$ HFs with that of Li^8 fragments it is found that light HFs are produced in the cascade-evaporation stage of disintegration of Ag and Br nuclei.

(ii) Contribution of deuterons and tritons to fast-charged particles, with residual range $\geqslant 4$ mm., from decay of NMHFs is $\lesssim 4\%$.

(iii) The energy spectrum of fast protons (energy $\geqslant 30$ MeV) from decay of NMHFs does not change significantly with the charge of the HFs.

(iv) The value of Q^- increases rapidly with the increase in charge of HF. The experimental value of Q^- for HFs with $Z \geqslant 3$ is $14{\cdot}6 \pm 3{\cdot}0$ and is significantly high compared to the theoretically calculated values.

(v) The value of S is greater than 1 for all charge groups of NMHFs.

ACKNOWLEDGEMENT

We are extremely grateful to Professor R. R. Daniel for helpful and stimulating discussions.

REFERENCES

1. Dalitz, R. H. ... *EFINS*, — 63-29.
2. Ferrari, E. and Fonda, L. *Nuov. Cim.*, 1958, **7**, 320.
3. Ganguli, S. N., Rao, N. K. and Swami, M. S. *Ibid.*, 1965, **36** (Part I), 33.
4. Burte, D. P., Ganguli, S. N., Rao, N. K., Ray, A. K., Rengarajan, T. N. and Swami, M. S. *Ibid.*, 1965, **36** (Part II), 733.
5. Burte, D. P. Chaudhari, K. N., Ganguli, S. N. Rao, N. K. and Swami, M. S. (Part IV). *Proc. Ind. Acad. Sci.*, 1966, **64 A**, 213.
6. Barkas, W. H. ... *Nuov. Cim.*, 1958, **8**, 201.
7. Fry, W. F. and White, G. R. *Phys. Rev.*, 1953, **90**, 207.
8. Heckman, H. H., Perkins, B. L., Simon, W. G., Smith, F. M. and Barkas, W. H. *Ibid.*, 1960, **117**, 544.
9. Chaudhari, K. N., Ganguli, S. N. and Rao, N. K. (Private Communication).
10. Jones, B. D., Sanjeevaiah, B., Zakrzewski, A., Csej they-Barth, M., Lagnaux, J. B., Sacton, J., Beniston, M. J., Burhop, E. H. S. and Davis, D. H. *Phys. Rev.*, 1962, **127**, 236.
11. Lemonne, J., *et al.* ... *Nuov. Cim.*, 1966, **41**, 235.
12. Burte, D. P., Chaudhari, K. N., Ganguli, S. N., Rao, N. K. and Swami. M. S. (Part III), *Proc. Ind. Acad. Sci.*, 1966, **64 A**, 203.

13. Ganguli, S. N., Rao, N. K. and Swami, M. S. — *Nuovo Cim.*, 1963, **28**, 1258.
14. Konig, L. A., Mattauch, J. H. E. and Wapstra, A. H. — *Nucl. Phys.*, 1962, **31**, 1.
15. Rosenfeld, A. H., Galtieri, A. B., Barkas, W. H., Bastien, P. L., Kirz, J. and Ross, M. — *UCRL*, 1965, 8030.
16. Chaudhari, K. N., Ganguli, S. N., Rao, N. K. and Swami, M. S. — *Proc. Ind. Acad. Sci.*, 1966, **64 A**, 51.
17. Burhop, E. H. S., Davis, D. H., and Zakrzewski, J. — *Progress in Nuclear Physics*, 1964, **9**, 225.
18. Gagarin, Yu. F. and Ivanova, N. S. — *Sov. Phys. JETP*, 1964, **18**, 1228.
19. Cüer, P. — *Proc. Int. Conf. on Hyperfragments CERN*, 1963, 641–123.
20. Schneps, J., Fry, W. F. and Swami, M. S. — *Phys. Rev.*, 1957, **106**, 1062.
21. Silverstein, E. M. .. — *Suppl. Nuov. Cim.*, 1958, **10**, 41.
22. Sacton, J. .. — *Ibid.*, 1960, **18**, 266.
23. Bhowmik, B., Goyal, D. P. and Yamdagni, N. K. — *Nucl. Phys.*, 1963, **48**, 652.
24. Holland, M. W. .. — *Nuov. Cim.*, 1964, **32**, 48.
25. Kenyon, I. R., Ismail, A. Z. M., Key, A. W., Lokanathan, S. and Prakash, Y. — *Ibid.*, 1964, **30**, 1365.
26. Ganguli, S. N. .. — *Ph.D. Thesis*, Bombay University, 1966.
27. Baldo-Ceolin, M., Dilworth, C., Fry, W. F., Greeing, W. D. B., Huzita, H., Limentani, S. and Sichirolla, A. E. — *Nuov. Cim.*, 1958, **7**, 328.
28. Berkovich, I. B., Zhdanov, A. P., Lepekhin, F. G. and Kokhlova, Z. S. — *Sov. Phys. JETP*, 1960, **11**, 311.
29. Gorge, V., Koch, W., Lindt, W., Nikolic, M., Subotic-Nikolic, S. and Winzeler, H. — *Nucl. Phys.*, 1960, **21**, 599.